Explore Spreading of Droplets with Computer Simulation

***Abstract*—In the realm of production and daily life, the collision phenomenon between droplets and objects is a focal point in the study of engineering fluid dynamics. The infiltration and spreading behavior of various types of droplets on solid and liquid surfaces constitute a prominent subject of investigation. The research outcomes in this domain find extensive applications in fields such as multiphase flows and thermal spray coating. However, due to the intricate nature of their dynamical states, probing into issues within this domain typically necessitates the utilization of computational methodologies from computer science for simulation, emulation, and analysis.**

To delve into the dynamical states of the droplet spreading process and address the pivotal influencing factors therein, this study devises a simplified model based on rational assumptions. Evolution models employing ordinary and partial differential equations are derived. Furthermore, incorporating finite element analysis techniques, the model undergoes simulation and analysis via computer experimental methods, leading to reasonably sound conclusions.

***Keywords*—Droplet impact, wetting properties, spreading, fluid dynamics model, numerical computation, finite element simulation, VOF**

I. INTRODUCTION

1.1 Background

The spreading process of droplets on flat surfaces is ubiquitous in daily life and holds significant importance in many industrial applications. From the minute raindrops spreading on window glass to the formation of ice on aircraft wings due to water droplet spreading during flight, and from industrial techniques such as the formation of water films on oil reservoir surfaces for fluid sealing to semiconductor device production, the phenomenon of droplet spreading on surfaces is indispensable[1]. Moreover, after establishing simplified models to describe the dynamic states, the complex numerical solution and simulation processes often require the assistance of computer science-related methods. Therefore, the dynamics of droplet spreading are subjects of interest and research in various fields such as physics, computer science, and engineering.

1.2 Problem posing

Assuming a droplet falls onto a surface with a certain initial velocity and gradually spreads on the surface. Influenced by gravity, surface tension, and viscous forces, the spreading process of the droplet can be mainly divided into stages such as inertial jumping, drainage/gas expulsion, rapid spreading, and stable spreading (as shown in Figure 1).

Fig. 1. Illustration of the droplet spreading process.

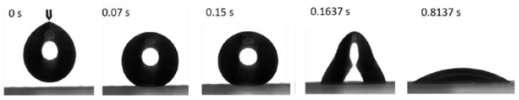

To deeply investigate the influencing factors of the droplet spreading process and apply them to practical industrial engineering, we will establish a mathematical model to explore the dynamic states and key influencing factors during the droplet spreading process, and address the following questions:

Question 1: A water droplet with a diameter of 100 micrometers starts falling from a stationary state closely to the surface, and eventually reaches a contact angle of 120 degrees with the surface. Model and solve the spreading process of the droplet to obtain its final stable static spreading state.

Question 2: Modify the initial stationary state of the water droplet in Question 1 to have a certain initial velocity, and determine the relationship between the droplet's falling velocity and the spreading process of the droplet.

Question 3: Change the solid surface in Questions 1 and 2 to a gasoline surface, and re-solve the above two questions to explore the differences in the results.t for the added nonlinearities.

1.3 Problem Analysis

During the spreading process, a droplet is primarily influenced by gravity, surface tension, and viscous forces. Fundamentally, the droplet spreading process is a fluid flow problem under the action of these three forces. Therefore, it satisfies the Navier-Stokes equations, and the entire process also inevitably complies with the conservation of energy equation, providing two approaches for problem-solving.

Considering the droplet's spherical shape and symmetry, we can select the vertical direction and any horizontal direction to form a two-dimensional plane, thus reducing the three-dimensional problem to a two-dimensional one for analysis. Research indicates that the static contact angle model alone cannot fully describe the dynamic spreading characteristics of fluid on solid surfaces. Therefore, the concept of wetting contact lines[2] (dynamic contact lines formed at the solid-liquid-gas three-phase contact interface when the droplet spreads along the solid wall), droplet spreading dynamic equations[3], and precursor films[4] are introduced. This paper will describe the spreading process using parameters such as

Thisr paper is submitted on March 22nd, 2024 for review. This work was supported in part by the professors from Department of Computer Science and Technology, Xi'an Jiaotong University.

film thickness (distance from the droplet's apex to the solid plane), spreading radius, and wetting contact lines.

Several factors influence the spreading process:

1. The properties of the solid plane affect surface tension and determine the contact angle at stability (final contact angle).
2. The size of the droplet affects gravity.
3. The viscosity of the droplet affects viscous forces.
4. The initial velocity of the droplet upon touching the solid plane affects the spreading process.
5. Additionally, the spreading conditions on both the solid and liquid surfaces will vary.

This paper will explore the impact of these factors on the droplet spreading process.

II. BEFORE STARTING

2.1 Basic Symbols

Symbol	Explanation
u_x	Velocity component in the X-direction
u_z	Velocity component in the Z-direction
p	Intensity of pressure
ρ	Density of the droplet
μ	Kinematic viscosity of the droplet
g	Acceleration due to gravity
$z=h(x,t)$	Two-dimensional contour curve of the droplet
R	Spreading radius of the droplet
β	Contact angle
σ	Surface tension coefficient of the droplet
d_0	Initial diameter of the droplet

2.2 Assumptions

(1) The characteristic scale of the liquid droplet in the horizontal direction is much larger than its characteristic scale in the vertical direction.

(2) Droplet spreading is primarily governed by surface tension and constitutes an isothermal motion of an incompressible Newtonian fluid.

(3) The initial state of the liquid droplet is spherical and possesses cylindrical symmetry. Therefore, the three-dimensional problem is reduced to a two-dimensional problem in the vertical direction and any horizontal direction.

(4) The diameter of the liquid droplet is approximately 0.1 mm, at which scale, the Bond number is very small. Hence, the influence of gravity can be neglected when considering droplet spreading on the solid surface.

(5) In the scenario of droplet collision with the solid surface, considering the droplet diameter and to avoid the phenomenon of complete fragmentation and splashing, it is assumed that the droplet velocity is not too high, ranging from 0 m/s to 1 m/s.

(6) The droplet does not mix with gasoline, and the density of the droplet (water droplet) is greater than the density of the liquid surface (gasoline).

(7) The diameter of the liquid droplet is still around 0.1 mm, and the initial velocity of the droplet colliding with the oil surface ranges from 0 m/s to 1 m/s. The oil pool is considered to be infinitely large and sufficiently deep.

III. IMPLEMENTION

3.1 Problem 1

3.1.1 Basis of dynamic equations

For the problem of droplet spreading along a horizontal wall with an initial velocity of 0, where the lower surface of the droplet is the solid substrate and the upper surface is the gas-liquid interface, both the effect of gravity and the surface tension at the free interface need to be simultaneously considered. For the sake of modeling convenience, we assume that the characteristic scale of the droplet in the horizontal direction is much larger than that in the vertical direction, and droplet spreading is dominated by surface tension, constituting an isothermal motion of an incompressible Newtonian fluid. Due to the aforementioned assumptions and the isotropic nature of droplet spreading in the horizontal direction considered in this problem, we can consider the problem in a two-dimensional plane. Below are the two-dimensional Navier-Stokes equations and continuity equation for droplet spreading:

$$\frac{\partial p}{\partial x}+\rho G_x=\mu\left(\frac{\partial^2 u_x}{\partial x^2}+\frac{\partial^2 u_x}{\partial z^2}\right) \quad (1)$$

$$\frac{\partial p}{\partial z}+\rho G_z=\mu\left(\frac{\partial^2 u_z}{\partial x^2}+\frac{\partial^2 u_z}{\partial z^2}\right) \quad (2)$$

$$\frac{\partial u_x}{\partial x}+\frac{\partial u_z}{\partial z}=0 \quad (3)$$

Where u_x and u_z are the velocity components of the droplet in the x and z directions, respectively. ρ is the liquid density,

μ is the kinematic viscosity of the droplet, P is the pressure, G_x and G_z are the accelerations due to gravity in the x and z directions, respectively.

The symbols for the various aspects of the droplet spreading process described above are indicated in Figure 2.

Fig. 2. Droplet spreading process.

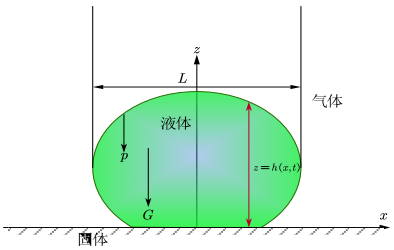

3.1.2 Boundary condition treatment

Boundary conditions at the solid-liquid interface: For the boundary conditions at the solid-liquid interface, we adopt the Navier linear slip boundary condition, which is represented as follows at z=0:

$$u_z = 0 \quad (4)$$

$$u_x = b\frac{\partial u_x}{\partial z} \quad (5)$$

In the above equations, b represents the slip length, defined as:

$$b = \frac{\upsilon_x \eta}{\tau} \quad (6)$$

Where υ_x is the velocity of the fluid in the x-direction, η is the dynamic viscosity of the fluid, and τ is the shear stress.

The Navier linear slip model established based on the linear slip boundary condition is illustrated in Figure 3.

Fig. 3. The Navier linear slip model.

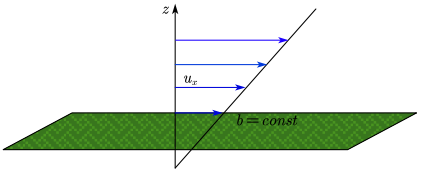

Boundary condition at the liquid-gas interface: At the interface between the liquid and gas $z = h(x,t)$, the velocity of the droplet in the z-direction is:

$$u_z = \frac{\partial z}{\partial t} = \frac{\partial h(x,t)}{\partial t} = u_x\frac{\partial h}{\partial x} + \frac{\partial h}{\partial t} \quad (7)$$

Furthermore, it is noted that at the interface between the liquid and gas, at $z = h(x,t)$, under the assumption of air having no viscosity, it is considered that the surface tension between the liquid and gas is continuous. Hence, we have:

$$\left.\frac{\partial u_x}{\partial z}\right|_{z=h} = 0 \quad (8)$$

Taking into account the Laplace-Young boundary condition at the interface between the liquid and gas, for a curved liquid surface, the presence of surface tension σ_g at the interface between the liquid and gas results in a pressure difference p on the two sides near the liquid surface. According to the Laplace pressure formula, the Laplace-Young boundary condition at the interface between the liquid and gas can be expressed as:

$$p = -\sigma_g \cdot \kappa \quad (9)$$

The various physical quantities in the above equation are indicated in the following diagram (Figure 4).

Fig. 4. Surface Laplace pressure of the droplet.

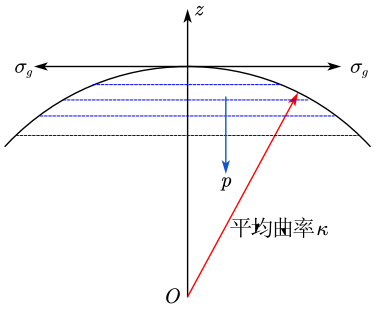

After non-dimensionalization and simplification, the differential equation for membrane thickness considering the curvature of the curved liquid surface is obtained:

$$\mu\frac{\partial h}{\partial t} - \frac{\partial}{\partial x}\left[\rho g\left(bh^2 + \frac{1}{3}h^3\right)\frac{\partial h}{\partial x}\right] + \frac{\partial}{\partial x}\left[\sigma_g\left(bh^2 + \frac{1}{3}h^3\right)\frac{\partial \kappa}{\partial x}\right] = 0 \quad (10)$$

Where, $\kappa = \frac{\frac{\partial^2 h}{\partial x^2}}{\left[1+\left(\frac{\partial h}{\partial x}\right)^2\right]^{\frac{3}{2}}}$

3.1.3 Numerical computation and solution.

The following numerical computation will be used to solve the differential equation for membrane thickness. Let t = 0 be the initial moment of the droplet spreading motion, at which the droplet just contacts the solid wall, forming a spherical droplet. Thus, we have:

$$h(x,0) = \sqrt{R^2 - x^2},\ -R \leqslant x \leqslant R \quad (11)$$

In the numerical simulation process, given the initial radius of the spherical droplet as $R = 50\mu m$, and assuming the actual spreading radius of the droplet is L_0, we have the relationship:

$$h(x,t) = 0,\ x = \pm L_0 \quad (12)$$

Based on the initial conditions and boundary conditions described above, a numerical calculation program will be written in Mathematica to obtain the results. The specific calculation process is illustrated in the flowchart shown in Figure 5.

Fig. 5. The Navier linear slip model.

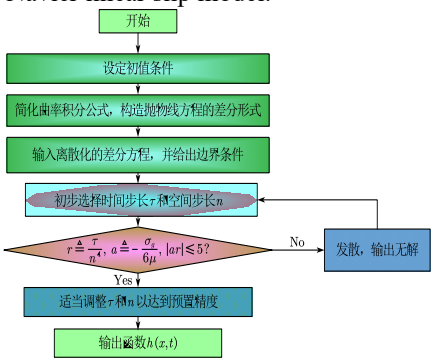

The spreading radius of the droplet can to some extent measure the degree of spreading of the droplet on the solid surface. Based on numerical calculations, the relationship between the spreading radius of the droplet on the solid surface and time can be plotted. Specifically, the spreading radius exhibits periodic oscillations with decay over time. The variation of the spreading radius within one period is illustrated in Figure 6:

Fig. 6. Graph showing the variation of the spreading radius of the droplet on the solid surface over time in the absence of initial velocity.

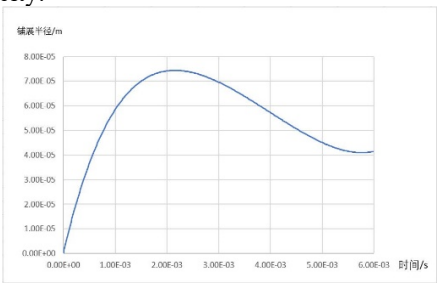

Additionally, numerical calculations can also be used to plot the relationship between the membrane thickness (height) of the droplet during spreading on the solid surface and time. Specifically, the membrane thickness exhibits periodic oscillations with decay over time, as shown in the Figure 7.

Fig. 7. Graph showing the variation of membrane thickness over time when the droplet has no initial velocity.

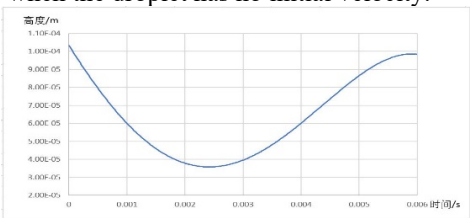

After obtaining the results from the calculations, they can be compared with the simulation results obtained using simulation software to validate the correctness of the model results.

Based on the results obtained from the model, further analysis reveals that for small droplets with a certain diameter (around 100 μm), the properties of the wall surface will have a significant impact on the spreading and recoiling processes of the droplet. When the wall surface becomes more hydrophobic, the surface tension coefficient of the droplet increases, resulting in a decrease in the final spreading radius and making it more prone to rebounding phenomena.

3.1.4 Verification of Simulation for Problem 1

We utilized the fluid dynamics module of the finite element simulation software Ansys Student 2021 R2, specifically Fluent, to perform simulation of the spreading process of the droplet without initial velocity. We selected liquid water and air as the two phases, employing the Volume of Fluid (VOF) multiphase flow model and laminar viscosity model. The parameters used in the multiphase flow model include the surface tension coefficient between water and air and the contact angle （120°） between solid and liquid. The working pressure of air was set to standard atmospheric pressure, the gravitational acceleration was set to g=9.81m/s^2, and the density was set to 1.225kg/m^3. Suitable volume parameters, coordinate parameters, and material parameters were assigned for element marking. Proper planes and contours were selected, and volume gradient parameters were set to record the animation.

Figure 8 below shows a portion of the simulation process for the droplet spreading without initial velocity. A final stable static contact angle of 120° has been set. It has been verified that the maximum height, spreading radius, and other relevant parameters have relative errors controlled within 10%, demonstrating a high level of agreement with the numerical solution.

Fig. 8. droplet spreading at different time points.

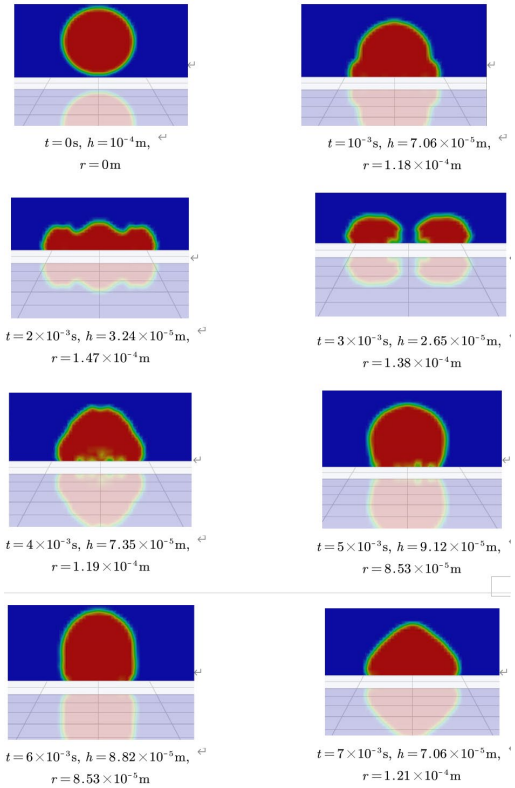

3.2 Problem 2

The entire impact process of the droplet can be divided into two stages. The first stage is the initial impact stage, during which the droplet deforms from a spherical shape when falling to a disk attached to the solid surface. The second stage is the expansion and contraction stage of the liquid, during which the liquid disk expands along the solid surface to its maximum diameter and then contracts to its final diameter.

3.2.1 Analysis of Kinetic Energy Loss during Initial Impact Stage

During the initial deformation, some of the initial kinetic energy of the droplet is dissipated due to molecular interactions inside the liquid. We define ζ as the impact coefficient to measure the kinetic energy loss during the deformation stage, which is given by the formula:

$$E_{k1} = \zeta E_{k0} \quad (13)$$

Where E_{k0} is the initial kinetic energy of the droplet and E_{k1} is the initial kinetic energy of the expanded liquid disk. For the value of ζ, according to Toda's experimental results[5], we have the following expression:

$$\zeta = e^{-0.083 \cdot u_0^{1.5}} \quad (14)$$

From this equation, we can deduce that when the collision velocity is 0, the impact coefficient is 1; when the collision velocity is 1 m/s the impact coefficient is approximately 0.92; when the collision velocity is 4 m/s, the impact coefficient is approximately 0.51. We consider that when the collision velocity is greater than 1 m/s, the energy loss cannot be ignored.

Fig. 9. Droplet impacting the solid surface

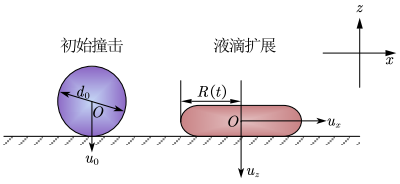

3.2.2 Detailed Analysis of Droplet Spreading Stage

After the initial impact stage, the liquid disk spreads outward from the collision center along the surface like a liquid film. According to the law of conservation of energy for the entire process, we have:

$$E_p + E_k + E_d = const \quad (15)$$

Where E_p is the surface energy of the liquid, E_k is the kinetic energy of the liquid disk, and E_d is the energy loss due to viscous motion inside the liquid. These three types of energy can be expressed respectively by the following formulas:

$$E_p = S_s\sigma_s + S_g\sigma_g \quad (16)$$

$$E_k = \frac{1}{2}\rho_l \int_0^V (u_z{}^2 + u_x{}^2) dV \quad (17)$$

$$E_d = \int_0^t \int_0^V \phi dt dV \quad (18)$$

Where S_s and S_g represent the contact areas between the liquid droplet and the solid wall, and between the liquid droplet and the air, respectively. σ_s and σ_g represent the effective surface tension coefficients between gas-liquid-solid and gas-liquid interfaces, respectively. \(\eta \) is the energy dissipation rate per unit volume of the droplet, which is given by:

$$\phi = \mu\left\{2\cdot\left[\left(\frac{\partial u_z}{\partial z}\right)^2 + \left(\frac{\partial u_x}{\partial x}\right)^2\right] + \left(\frac{\partial u_z}{\partial z} + \frac{\partial u_x}{\partial x}\right)^2 - \frac{2}{3}\cdot\left(\frac{\partial u_z}{\partial z} + \frac{\partial u_x}{\partial x}\right)^2\right\} \quad (19)$$

Where μ is the dynamic viscosity of the droplet.

The spreading process of the droplet along the wall surface is similar to the flow of the droplet toward the surface, hence the following velocity distribution expressions:

$$u_z = -\frac{2}{n+1} c z^{n+1} \quad (20)$$

$$u_x = c x z^n \quad (21)$$

These expressions satisfy the continuity equation of the liquid:

$$\frac{1}{x}\frac{\partial}{\partial x}(x u_x) + \frac{\partial u_z}{\partial z} = 0 \quad (22)$$

By selecting different constants n, both zero velocity and zero shear stress boundary conditions can be satisfied.

Whether the droplet wets the solid surface or not depends on the relative magnitude of the interaction force between the liquid molecules and the solid molecules (called adhesion) and the interaction force between the liquid molecules (called cohesion). We discuss the impact situation of the droplet in two scenarios: wetting contact and non-wetting contact (for detailed analysis, refer to Appendices). The differential equations for the spreading process under wetting and non-wetting contact conditions are given as follows:

Differential equation for wetting contact:

$$\frac{d^2R}{dt^2}\cdot\left(\frac{3}{20} + \frac{d_0{}^6}{378R^6}\right) - \left(\frac{dR}{dt}\right)^2\cdot\frac{d_0{}^6}{126R^7} + \frac{2\sigma R(1+\cos\beta)}{d_0{}^3\rho_l} - \frac{\sigma}{3\rho_l R^2} + \left(\frac{36R^4}{d_0{}^6} + \frac{14}{5R^2}\right)\cdot\frac{\mu}{\rho_l}\frac{dR}{dt} = 0 \quad (23)$$

Differential equation for non-wetting contact:

$$\left(\frac{d_0{}^6}{162R^6} + \frac{1}{12}\right)\frac{d^2R}{dt^2} - \frac{d_0{}^6}{54R^7}\left(\frac{dR}{dt}\right)^2 + \frac{6\sigma R}{\rho_l d_0{}^3} - \frac{\sigma}{3\rho_l R^2} = 0 \quad (24)$$

3.2.3 Numerical Solution for Both Scenarios

We used MATLAB to numerically solve the ordinary differential equations (23) and (24) for different initial conditions. This allowed us to obtain the variation of the

spreading radius of the droplet over time for each scenario. The program codes are provided in the appendix.

The results indicate that after the droplet impacts the surface, it exhibits damping oscillatory characteristics, with the spreading radius of the droplet showing a decay oscillation over time.

Wetting Contact: For the wetting contact scenario, by solving equation (23) for a water droplet with a diameter of 100 μm, and substituting different initial velocities, we can obtain numerical solutions for the variation of the spreading radius R over time t. The graph below (Figure 10) illustrates the spreading radius of the droplet over time for different initial collision velocities:

Fig. 10. Graph showing the variation of spreading radius over time for different velocities in wetting contact scenario

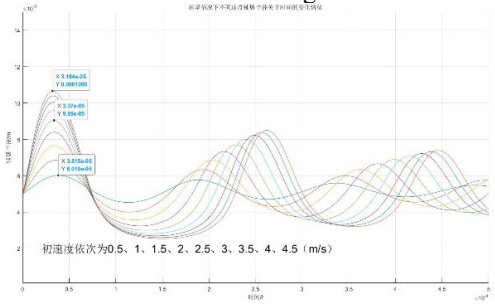

The graph displays the spreading radius of the droplet over time, with initial velocities ranging from 0.5 to 4.5 m/s at intervals of 0.5. It is observed that higher initial velocities result in larger oscillations in the spreading radius.

Non-wetting Contact: The discussion for the non-wetting contact scenario is similar to the wetting contact scenario. By solving equation (24) for a water droplet with a diameter of 100 μm and substituting different initial velocities, we can obtain numerical solutions for the variation of the spreading radius R over time t. The graph below (Figure 11) illustrates the spreading radius of the droplet over time for different initial collision velocities:

Fig. 11. Graph showing the variation of spreading radius over time for different velocities in non-wetting contact scenario

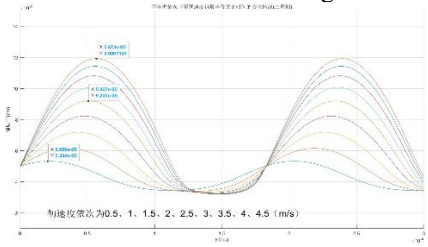

The graph displays the spreading radius of the droplet over time, with initial velocities ranging from 0.5 to 4.5 m/s at intervals of 0.5. The analysis of the graph indicates that the spreading radius decay is much slower in the non-wetting contact scenario compared to the wetting contact scenario. Therefore, only the variation for the first two oscillation cycles is depicted. This is attributed to the smaller dissipation energy between the liquid and the surface in the non-wetting contact scenario.

3.2.4 Validation of Simulation for Problem 2

Following a similar simulation process as in Problem 1, with modifications only to the initial velocity parameters of the droplet upon collision, we used the Ansys Fluent module to simulate the spreading process of a droplet with initial velocity. The simulation results were then compared with the numerical analysis results, confirming the accuracy of the model.

Fig. 12. Simulation process of droplet collision with solid surface with initial velocity

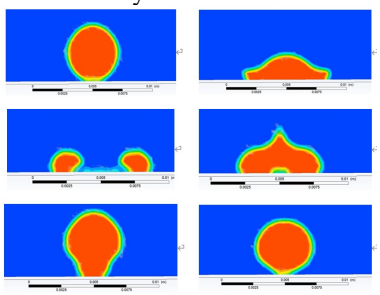

3.3 Problem 3

3.3.1 Discussion and Condition Specification of the Problem Scenario

Based on relevant simulations and experiments, when the droplet size is too large and the impact velocity is too fast, the droplet will shatter into small droplets and splash[6]:

Fig. 13. Droplet with a velocity of 4 m/s and diameter of 3.55 mm impacting an oil film

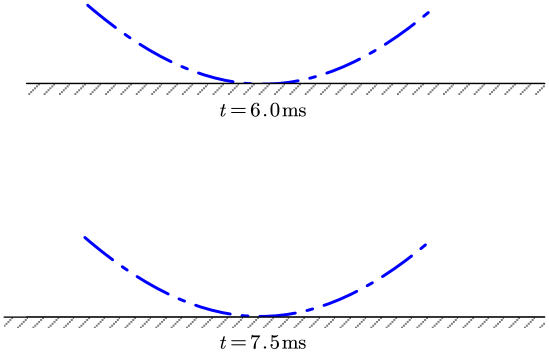

Additionally, if the oil pool is too shallow, it will first form a cylindrical void, followed by the formation of a crown-like structure. Subsequently, under the influence of gravity, the crown structure collapses, and after reaching its maximum size, the void also contracts due to the surface tension and viscosity forces, leading to the surrounding liquid squeezing inward. Finally, the mechanical energy contained in the entire system will cause the liquid in the oil pool to rush out of the oil-air interface, forming a long and thin liquid column. This entire process is referred to as the "crater-jet" process [7]:

Fig. 14. Schematic diagram of the "crater-jet" process

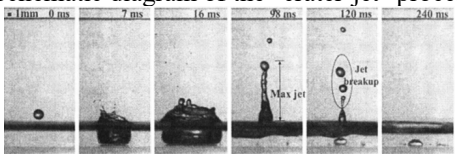

These two phenomena are clearly far from the spreading phenomenon we are studying. To avoid their occurrence, we need to specify the discussion conditions for Problem 3: the droplet size is still around 0.1 mm, the initial velocity of the droplet upon collision with the oil surface is between 0 and 1 m/s, and the oil pool is considered infinite and sufficiently deep.

3.3.2 Qualitative Analysis and Prediction of Spreading Results

During problem analysis, it was mentioned that due to the presence of the droplet's own gravity and kinetic energy, the oil-air interface (the interface between the oil pool and the air) will deform and shatter under the pressure of the droplet. At this point, the spreading surface is a complex and oscillating surface that changes over time. Below, we analyze the behavior of the oil pool liquid and the droplet during spreading.

For the oil pool liquid, initially, the central area of impact will be depressed by the droplet's impact, while small splashes will form at the edges. According to the discussion conditions, the droplet's velocity and size are small, so its momentum and impact force are also small. The Weber number is likewise small, and surface tension dominates over inertia. Therefore, the growth rate of the splashes is slow, and the splashes are relatively short. Subsequently, the splashes collapse under gravity, and the edge region sinks. At this point, due to the decreasing pressure in the central area, caused by the droplet's pressure, the central area begins to rise. Simultaneously, such disturbances propagate outward in the form of water waves. Afterwards, every point on the oil-air interface will undergo a decay oscillation motion [8].

For the droplet, after contacting the oil pool surface, under the influence of gravity and inertia, one side sinks into the oil pool while the other forms a water-oil mixture through the oil-air interface until the entire droplet is submerged in the gasoline. Since water has a higher density than gasoline, even if the initial velocity is zero, the droplet can still completely pass through the oil-air interface. Subsequently, due to gravity, the droplet will gather towards the lower end. At this point, the droplet is subject to gravity, inertia, and surface tension at the oil-air interface, resulting in a spindle shape. If the droplet's size is slightly larger, the sum of gravity and inertia will be more significant, causing the droplet to fracture during oscillation, with the upper part "inverted" and adhering to the oil-air interface (oil side), while the lower part deposits at the bottom of the container. If the sum of gravity and inertia is not sufficient to tear the droplet apart, then the entire droplet will adhere to the oil-air interface (oil side). Finally, the amplitude of the oil-air interface tends to zero, and the droplet reaches a stable spreading state below the oil-air interface. Considering that gasoline is hydrophobic and the oil pool surface is non-wetting, the contact angle is greater than 90°.

In summary, we make the following predictions for the final spreading state: in Case 1, where the droplet size is small and the collision velocity is low, the droplet will adhere to the underside of the oil pool surface as a whole, similar to the non-wetting spreading situation on a solid surface in Problem 1; in Case 2, where the droplet size is slightly larger and the collision velocity is slightly higher, the droplet will split in half, with the upper part adhering to the underside of the oil pool surface.

3.3.3 Simulation and Verification of Problem 3

We used the Ansys Fluent module to simulate the spreading process of a droplet with initial velocity on the oil surface. The process is as follows: select liquid water, air, and liquid gasoline as the three phases, use the multiphase flow model (VOF) and laminar viscosity model, with parameters including surface tension coefficients between water-air, water-gasoline, and air-gasoline, set the air working pressure to standard atmospheric pressure, working gravity to $g=9.81 m/s^2$, working density to $1.225 kg/m^3$, initialize the space as air and oil pool, set appropriate volume, coordinate, and material parameters for the unit marker, select appropriate plane and cloud maps, and set volume gradient parameters to record animations.

The figures below (Figures 15 and 16) respectively show part of the simulation process of a droplet with initial velocity spreading on the gasoline surface, with and without droplet fragmentation.

Fig. 15. The spreading of droplet with certain initial velocity on the surface of gasoline (without droplet fragmentation)

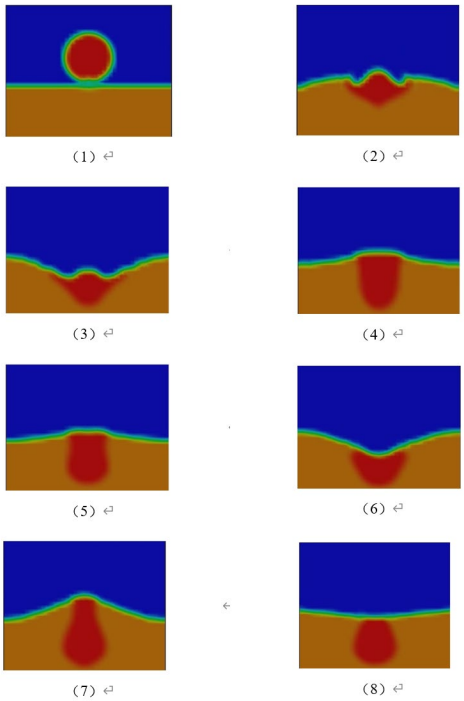

Fig. 15. The spreading of droplet with certain initial velocity on the surface of gasoline (with droplet fragmentation)

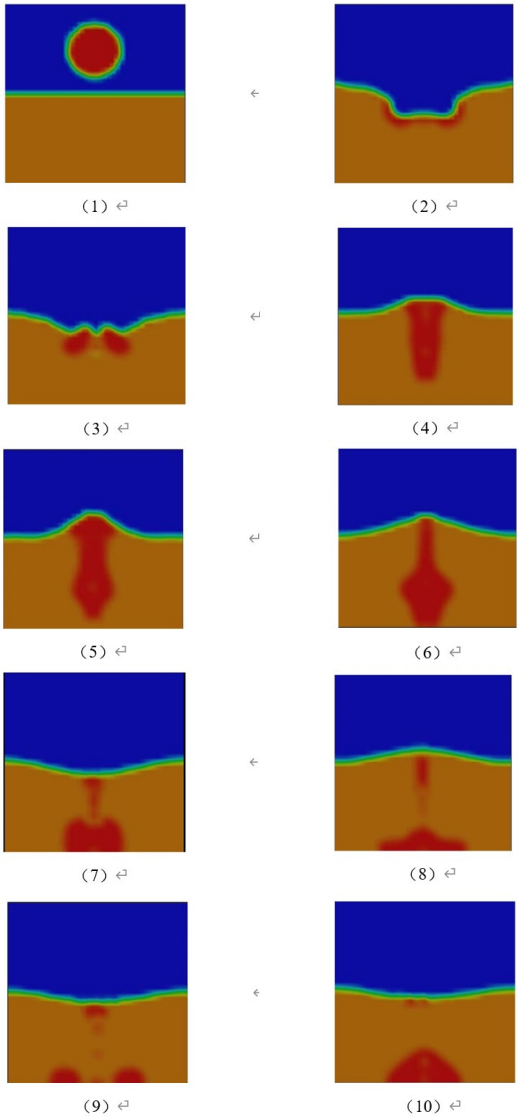

IV. CONCLUSION

4.1 Advantages of the Model and Paper

(1) Reasonable Assumptions: Based on extensive literature review, this paper establishes a series of scientifically reasonable assumptions, neglecting minor contradictions that have little impact on the modeling results. With a significant simplification of the model and algorithm, the paper achieves considerable modeling results.

(2) Rigorous Modeling: The paper rigorously discusses different models for different impact surface media and different initial velocities of droplet collisions, ensuring the distinct physical mechanisms of various models and accurate applicability conditions.

(3) Scientific Computation: Numerical solution methods are employed in the model solving process, with timely adjustments of relevant parameters, ensuring more reliable analysis of droplet states.

(4) Accurate Simulation: By using Ansys Fluent software and accurately defining droplet boundaries and initial parameters, the simulation is effectively conducted, resulting in high precision of the final simulation results.

4.2 Further Model Improvement:

(1) The model can only accurately compute the changes of parameters such as droplet film thickness and spreading radius over time for relatively small initial velocities (approximately less than [threshold]). When the initial velocity of the droplet is large, the model's error becomes significant.

(2) The loss of kinetic energy during the initial collision stage of the droplet is based on empirical formulas and lacks a deeper quantitative analysis.

REFERENCES

[1] Becker J, Grun G 2005 J. Phys.: Condens. Mat. 17 291
[2] Blake T D 1969 J. Colloid Interf. Sci. 299 1
[3] Oron A, Davis S H, Bankoff S G 1997 Rev. Mod. Phys. 69 931
[4] de Gennes P G 1985 Rev. Mod. Phys. 57 827
[5] 贺征, 郜冶, 顾璇,等. 液滴与壁面碰撞模型研究[J]. 哈尔滨工程大学学报, 2009, 30(3):267-270.
[6] 马理强, 刘谋斌, 常建忠,等. 液滴冲击液膜问题的光滑粒子动力学模拟[J]. 物理学报, 2012(24):000346-355.
[7] 范绪君. 水滴撞击油池动力学特性研究[D]. 合肥工业大学.
[8] 梁超. 微小液滴撞击固体壁面及薄液膜动态特性的数值研究[D]. 重庆大学, 2013.

Code for Question 1

```
solution=NDSolve[{0.00114*D[h[x,t],t]+D[1/3*h^3*72.75*2*10^-
3*D[D[h[x,t],x,x]/(1+(D[h[x,t],x])^2)^1.5,x],x]==0,h[x,0]==((5*10^-5)^2-x^2),h[x,0]==-((5*10^-5)^2-x^2),h[25*3^0.5*10^-
6,t]==0,h[-25*3^0.5*10^-6,t]==0},h[x,t],{x,-5*10^-5,5*10^-5},{y,0,6*10^-3}]
Plot3D[Evaluate[h[x,t]]/.First[solution]],{x,-5*10^-5,5*10^-5},{y,0,6*10^-3}]
```

Code for Question 2

解微分方程

```
function dy=func2(~,f)
dy=[0;0];
dy(1)=f(2);
dy(2)=(f(2))^2*(1E-4)^6/54/f(1)^7-6*0.073/1000*f(1)/(1E-4)^3+0.073/1000/3/f(1)^2;
end
function dy=func1(~,f)
dy=[0;0];
dy(1)=f(2);
dy(2)=((f(2))^2*(1E-4)^6/126/f(1)^7-2*0.073*f(1)*1.2/(1E-4)^3/1000+0.073/3/1000/(f(1))^2-
0.001/1000*f(2)*(36*(f(1))^4/(1E-4)^6+14/5/(f(1))^2))/(3/20+(1E-4)^6/378/f(1)^6);
end
```

主程序

```
options=odeset('RelTol',1E-8,'AbsTol',[1E-8,1E-8]);
figure(1)
for i=1:9
hold on;
y10=5E-5;
y20=(0.518*exp(-0.083*(i*0.5)^1.5))^0.5*(i*0.5);
[xi,yi]=ode45('func1',[0,2E-4],[y10,y20],options);
plot(xi,yi(:,1));axis([0 2E-4 1E-6 1.5E-4]);
end
text(2E-5,2E-5,'初速度依次为0.5、1、1.5、2、2.5、3、3.5、4、4.5（m/s）','FontSize',20);
grid on;
title('润湿情况下不同速度铺展半径关于时间的变化情况(二周期)');
xlabel('时间/t');
ylabel('铺展半径/m');
figure(2)
for i=1:9
hold on;
y10=5E-5;
y20=(0.518*exp(-0.083*(i*0.5)^1.5))^0.5*(i*0.5);
[xi,yi]=ode45('func1',[0,5E-4],[y10,y20],options);
plot(xi,yi(:,1));axis([0 5E-4 1E-6 1.5E-4]);
end
text(2E-5,2E-5,'初速度依次为0.5、1、1.5、2、2.5、3、3.5、4、4.5（m/s）','FontSize',20);
grid on;
title('润湿情况下不同速度铺展半径关于时间的变化情况');
xlabel('时间/t');
ylabel('铺展半径/m');
figure(3)
for i=1:9
hold on;
y10=5E-5;
```

```
y20=(0.348*exp(-0.083*(i*0.5)^1.5))^0.5*(i*0.5);
[xi,yi]=ode45('func2',[0,3E-4],[y10,y20],options);
plot(xi,yi(:,1));axis([0 3E-4 1E-5 1.5E-4]);
end
text(2E-5,2E-5,'初速度依次为0.5、1、1.5、2、2.5、3、3.5、4、4.5（m/s）','FontSize',20);
grid on;
title('不润湿情况下不同速度铺展半径关于时间的变化情况(二周期)');
xlabel('时间/t');
ylabel('铺展半径/m');
```

Discussion on Wetting Contact between Droplets and Solid Surfaces

When the surface temperature is lower than the liquid's saturation temperature, the liquid wets the surface, resulting in wetting contact. In this situation, n must be greater than 0, thus satisfying the following boundary conditions.

$$\begin{cases} x=0,\ u_x=0; \\ x=R,\ u_x=u_R=\dfrac{dR}{dt}; \\ z=0,\ u_z=0. \end{cases}$$

Regression analysis indicates that n=2 provides relatively ideal results. We express each velocity component using the average perimeter velocity of the liquid droplet disk:

$$u_x=\frac{3}{Rb^2}\frac{dR}{dt}xz^2$$

$$u_z=-\frac{2}{Rb^2}\frac{dR}{dt}z^3$$

where b is the instantaneous thickness of the liquid disk. Substituting yields the expression for kinetic energy:

$$b\triangleq\frac{{d_0}^3}{6R^2}$$

$$E_k=\pi\rho_l\left(\frac{9}{20}bR^2+\frac{2}{7}b^3\right)\cdot\left(\frac{dR}{dt}\right)^2$$

where ρ_l is the density of the droplet. In the case of wetting contact, the upper surface and periphery of the liquid droplet disk are in contact with air, and the bottom is in contact with the solid wall with a contact angle of β. Therefore, the surface energy is:

$$S_s\sigma_s=\pi R^2\sigma\cos\beta$$

$$S_g\sigma_g=(2\pi Rb+\pi R^2)\sigma$$

At time t, the dissipated energy equals the total dissipation accumulated from time zero to time t. Substituting yields Φ, further calculated as:

$$E_d=\frac{84}{5}\pi\mu\int_0^t\left(\frac{5}{14}\frac{R^2}{b}+b\right)\left(\frac{dR}{dt}\right)^2dt$$

Taking the instant of impact as the starting point in time, the initial instantaneous velocity of the liquid droplet disk can be solved simultaneously to be:

$$\left(\frac{dR}{dt}\right)\Big|_0=\sqrt{0.518\zeta}\,u_0$$

The initial radius can be approximated as:

$$R_0=\frac{d_0}{2}$$

Substituting and differentiating both sides, we obtain the differential equation describing the spreading process under wetting contact conditions as:

$$\frac{d^2R}{dt^2}\cdot\left(\frac{3}{20}+\frac{{d_0}^6}{378R^6}\right)-\left(\frac{dR}{dt}\right)^2\cdot\frac{{d_0}^6}{126R^7}+\frac{2\sigma R(1+\cos\beta)}{{d_0}^3\rho_l}-\frac{\sigma}{3\rho_lR^2}+\left(\frac{36R^4}{{d_0}^6}+\frac{14}{5R^2}\right)\cdot\frac{\mu}{\rho_l}\frac{dR}{dt}=0$$

Discussion on Non-Wetting Contact between Droplets and Solid Surfaces

There are various ways to achieve non-wetting contact between a liquid and a solid surface, such as mercury directly achieving non-wetting contact on a glass surface. In fact, when the surface temperature of the solid is much higher than the liquid's saturation temperature, a thin layer of vapor separates the liquid droplet disk from the solid flat surface after collision, also resulting in non-wetting contact. This phenomenon is known as the Leidenfrost Effect, as shown in the figure below. Although the process of achieving non-wetting contact varies, the kinetic analysis of the non-wetting contact result can be uniformly solved.

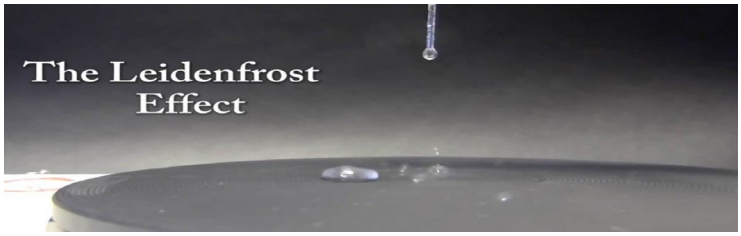

$$u_x = \frac{x}{R} \cdot \frac{dR}{dt}$$

$$u_z = -\frac{2}{R}\frac{dR}{dt} \cdot z$$

Therefore, the expressions for kinetic energy and the initial spreading velocity are:

$$E_k = \pi \rho_l \left(\frac{bR^2}{4} + \frac{2}{3} b^3 \right) \cdot \left(\frac{dR}{dt} \right)^2$$

$$\left(\frac{dR}{dt} \right) \Big|_0 = \sqrt{0.348\zeta}\, u_0$$

To derive the formula for surface energy at this point, note that during the expansion process, the upper surface of the liquid droplet disk forms a wavy surface. We approximately consider such a surface as a spherical wave in a state of micro-amplitude vibration, thus representing the surface energy approximately as:

$$S_s \sigma_s = 0$$

$$S_g \sigma_g = (2\pi R b + 3\pi R^2)\sigma$$

The dissipated energy is:

$$E_d = \frac{28}{3} \pi \mu \int_0^t b \left(\frac{dR}{dt} \right)^2 dt$$

Combining formulas, we obtain the differential equation describing the spreading process under non-wetting conditions as:

$$\left(\frac{{d_0}^6}{162R^6} + \frac{1}{12} \right) \frac{d^2R}{dt^2} - \frac{{d_0}^6}{54R^7} \left(\frac{dR}{dt} \right)^2 + \frac{6\sigma R}{\rho_l {d_0}^3} - \frac{\sigma}{3\rho_l R^2} = 0$$